Supplementary information for

Synthesis and catalysis of Co13 disk surrounded by vanadium-oxygen crown

Yuji Kikukawa,[*a] Isshin Yoshida,[a] Ryoji Mitsuhashi,[b] Masaru Yamane [a] and Yoshihito Hayashi[*a]

[a]*Department of Chemistry, Graduate School of Natural Science and Technology, Kanazawa University, Kakuma, Kanazawa 920-1192, Japan.*
E-mail: kikukawa@se.kanazawa-u.ac.jp
[b]*Institute of Liberal Arts and Science, Kanazawa University, Kakuma, Kanazawa 920-1192, Japan.*

Experimental Section

Instruments: NMR spectra were recorded with JEOL JNM-LA400. IR spectra were measured on Jasco FT/IR-4200 using KBr method. Elemental analyses of C, H, and N were performed by the Research Institute for Instru-mental Analysis at Kanazawa University. Electrospray ionization mass spectra were measured with JEOL JMS-T100TD. UV-vis spectra were measured on Jasco V770. Thermogravimetry data were collected on a Rigaku Thermo plus EVO2 instrument with a temperature sweep rate of 10 °C/min under 0.2 L/min N_2 flow. GC analysis was performed on Shimadzu GC-2014 and GC-2050 with a flame ionization detector (FID) equipped with ZB-WAXplus capillary columns (phenomenex, internal diameter = 0.25 mm, length = 30 m) and SH-PolarWax capillary column (Shimadzu, internal diameter = 0.25 mm, length = 30 m). GC-MS spectra were measured on Shimadzu GCMS-QP2010. An ALS/CH Instruments electrochemical analyzer (Model 600A) was used for voltammetric experiments under N_2 gas flow condition. The working electrode was glassy carbon, the counter electrode was Pt wire, and the reference electrode was Ag/Ag^+. The voltage scan rate was set at 100 mV s^{-1}. The concentration of the sample and the recrystalized supporting electrolyte, $\{n\text{-}Bu_4N\}PF_6$ was 1 mM and 100 mM, respectively. The potentials in all voltammetric experiments were converted using data derived from the oxidation of ferrocene (Fc/Fc^+, Fc = ferrocene) as an external reference. The distillation of the small amount of reagent was performed by glass tube oven SIBATA GTO-1000. Direct current magnetic susceptibilities of polycrystalline samples were measured on a Quantum Design SQUID magnetometer operating between 2 K and 300 K under a 1000 Oe magnetic field. Dynamic magnetic measurement was performed with a Quantum Design MPMS-XL7 SQUID magnetometer with ac fields of 3 Oe magnitude.

Reagents: Solvents and reagents were commercially available and used as received unless otherwise specified. 2-Butanol was dehydrated with molecular sieves 3A. Benzyl alcohol, benzaldehyde and 2-cyclohexene-1-ol were distilled just before use.

X-ray Crystallographic analysis: Single-crystal structural analysis was performed at –183°C with a Bruker D8 VENTURE diffractometer with Cu-*K*α radiation (λ = 1.54178 Å). The data reduction and absorption correction were completed using the APEX3 program.[S1] The structural analyses were performed using APEX3 and winGX for Windows software.[S2] All structures were solved by SHELXT (direct methods) and refined by SHELXL-2019/3.[S3] Non-hydrogen atoms were refined anisotropically. Hydrogen atoms are positioned geometrically and refined using a riding model.

Catalytic reaction: Substrate 1 mmol, catalyst 2-26 μmol, acetonitrile 1 mL, propylene carbonate 1 mL were put in the glass test tube with the screw cap. For GC analysis, internal standard naphthalene or chlorobenzene 0.2 mmol were added. The solution was kept at 32 °C. The solution was stirred at 800 rpm with the Teflon-coated magnetic stir bar. The reaction started with the addition of TBHP in decane solution 1 mmol to the reaction solution. Yields were determined by GC with internal standard method. The products were determined by the retention time of the commercially available authentic chemicals unless otherwise mentioned. After the reaction, the catalyst was collected by addition of excess amount of diethyl ether and filtration. The collected solids were characterized by IR or ^{51}V NMR spectroscopic analysis.

Additional references:

S1. *APEX3, SAINT, and SADABS, Bruker AXS Inc., Madison, Wisconsin, USA, 2015.*
S2. L. J. Farrugia, *J. Appl. Crystallogr.*1999, **32**, 837.
S3. G. M. Sheldrick, *Acta Crystallogr.* 2015, C71, 3.

Table S1. Crystallographic data for **Co13**.

formula	$C_{112}H_{206}Co_{13}N_{10}O_{92}S_8V_{24}$
fw	5409.99
crystal system	trigonal
space group	R –3 (#148)
a (Å)	33.1589(6)
b (Å)	33.1589(6)
c (Å)	15.9534(3)
V (Å^3)	15190.9(6)
Z	3
μ (mm^{-1})	18.403
R_1 ($I > 2\sigma(I)$)	0.0636
wR_2	0.2004

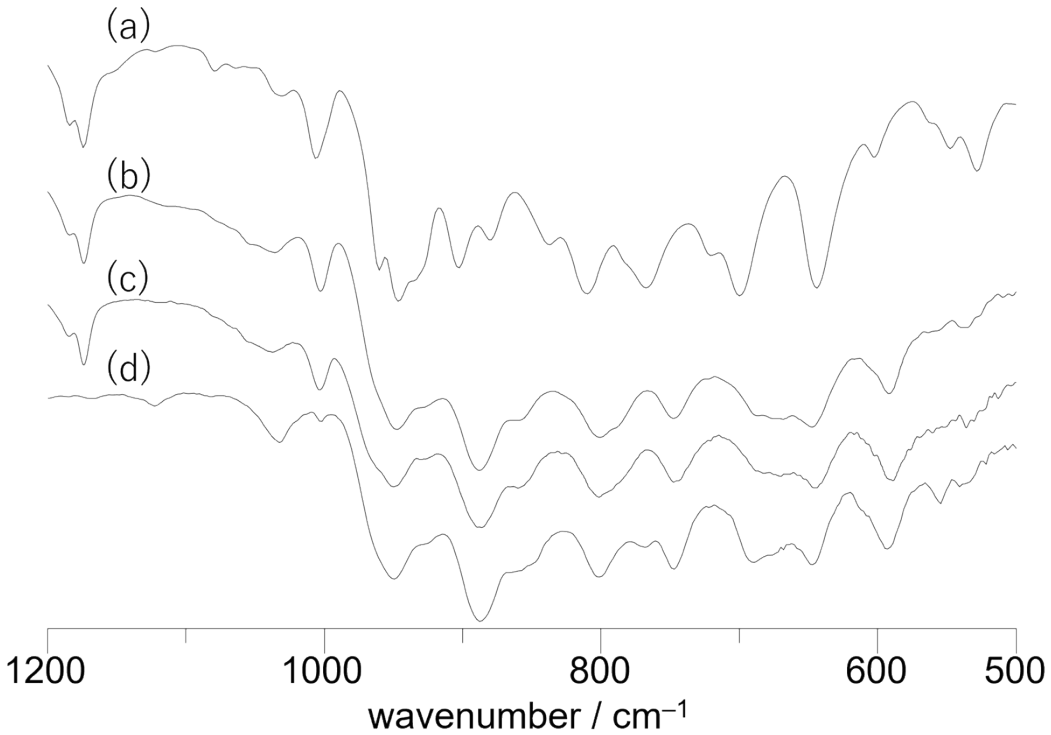

Figure S1. IR spectra of (a) **Co2**, (b) tetraethyl ammonium salts of **Co13** synthesized without addition of triethylamine, (c) tetraethyl and triethyl ammonium salts of **Co13** synthesized with addition of triethylamine and (d) trimethylphenyl ammonium salts of **Co13**.

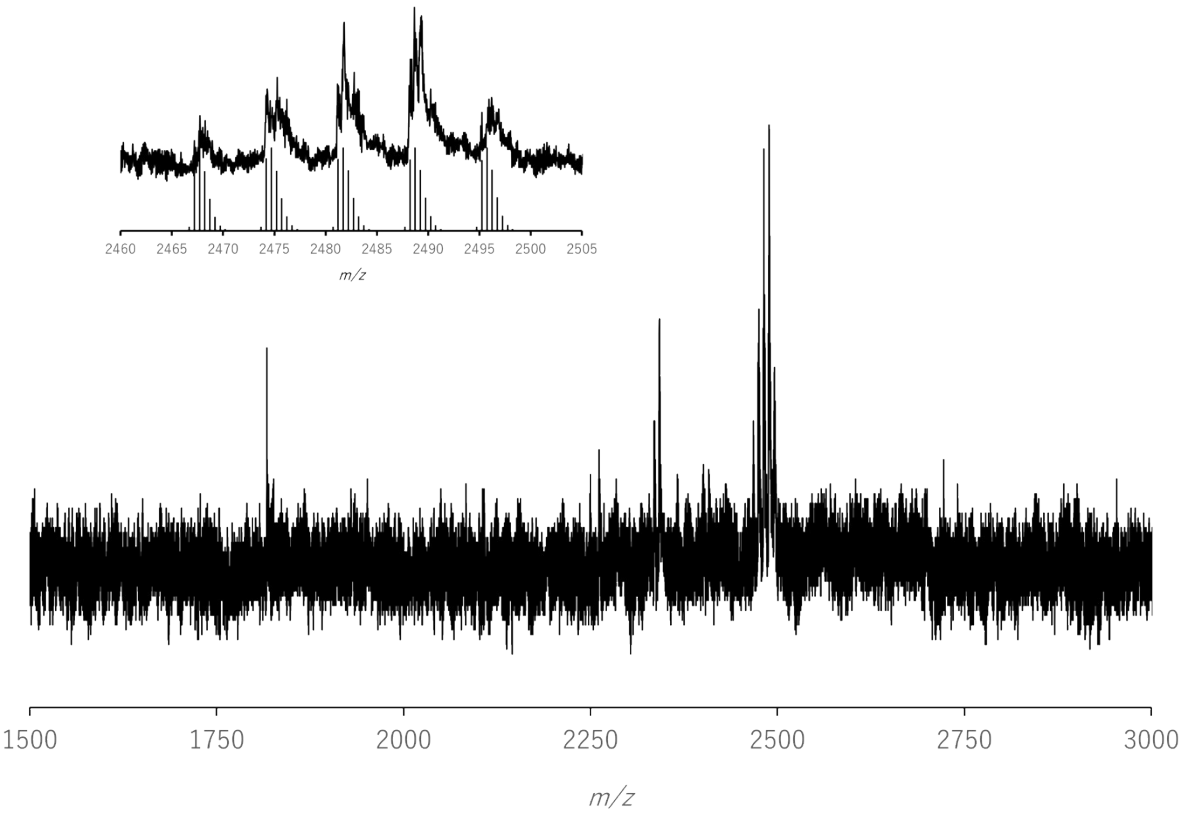

Figure S2. Electrospray ionization mass spectrum of **Co13** synthesized with addition of triethylamine. The insertion represents the expanded spectrum and the simulation. Peak sets at 2335, 2342, 2468, 2475, 2482, 2489, and 2496 were assignable to $\{(Et_4N)(HEt_3N)_{11}[Co_{13}(OH)_7(OMe)_5V_{24}O_{72}]\}^{2+}$, $\{(Et_4N)(HEt_3N)_{11}[Co_{13}(OH)_6(OMe)_6V_{24}O_{72}]\}^{2+}$, $\{(Et_4N)_{12}[Co_{13}(OH)_{10}(OMe)_2V_{24}O_{72}]\}^{2+}$, $\{(Et_4N)_{12}[Co_{13}(OH)_9(OMe)_3V_{24}O_{72}]\}^{2+}$, $\{(Et_4N)_{12}[Co_{13}(OH)_8(OMe)_4V_{24}O_{72}]\}^{2+}$, $\{(Et_4N)_{12}[Co_{13}(OH)_7(OMe)_5V_{24}O_{72}]\}^{2+}$, $\{(Et_4N)_{12}[Co_{13}(OH)_6(OMe)_6V_{24}O_{72}]\}^{2+}$, respectively.

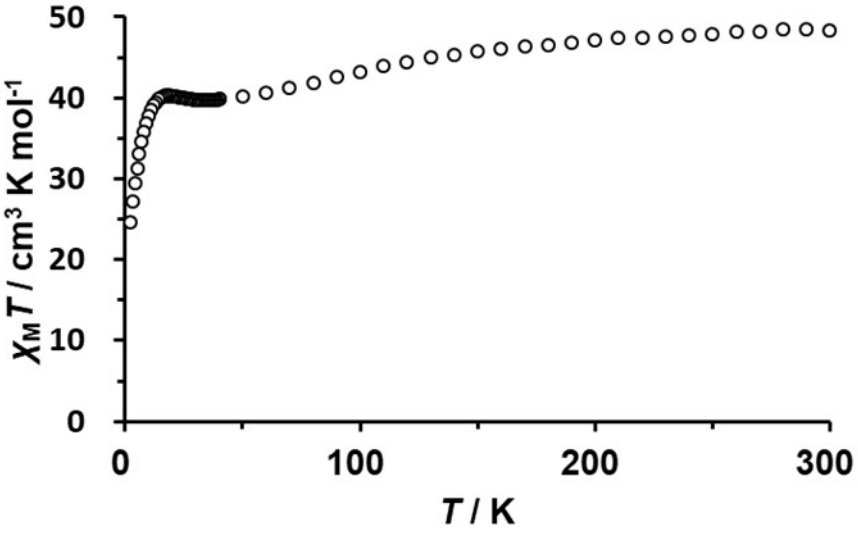

Figure S3. Temperature dependence of $\chi_M T$ values of **Co13** in the temperature range of 2–300 K under the magnetic field of 1000 Oe.

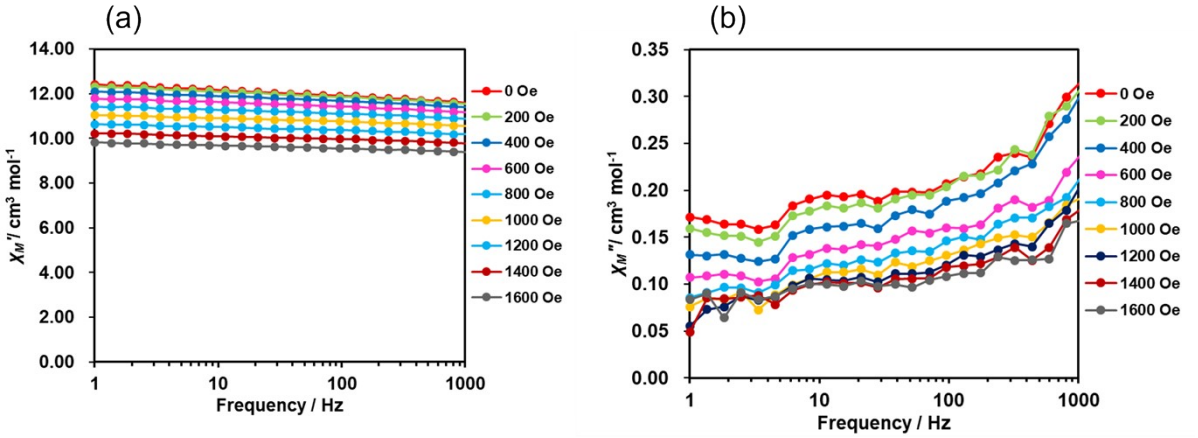

Figure S4. (a) In-phase and (b) out-phase susceptibility of **Co13**.

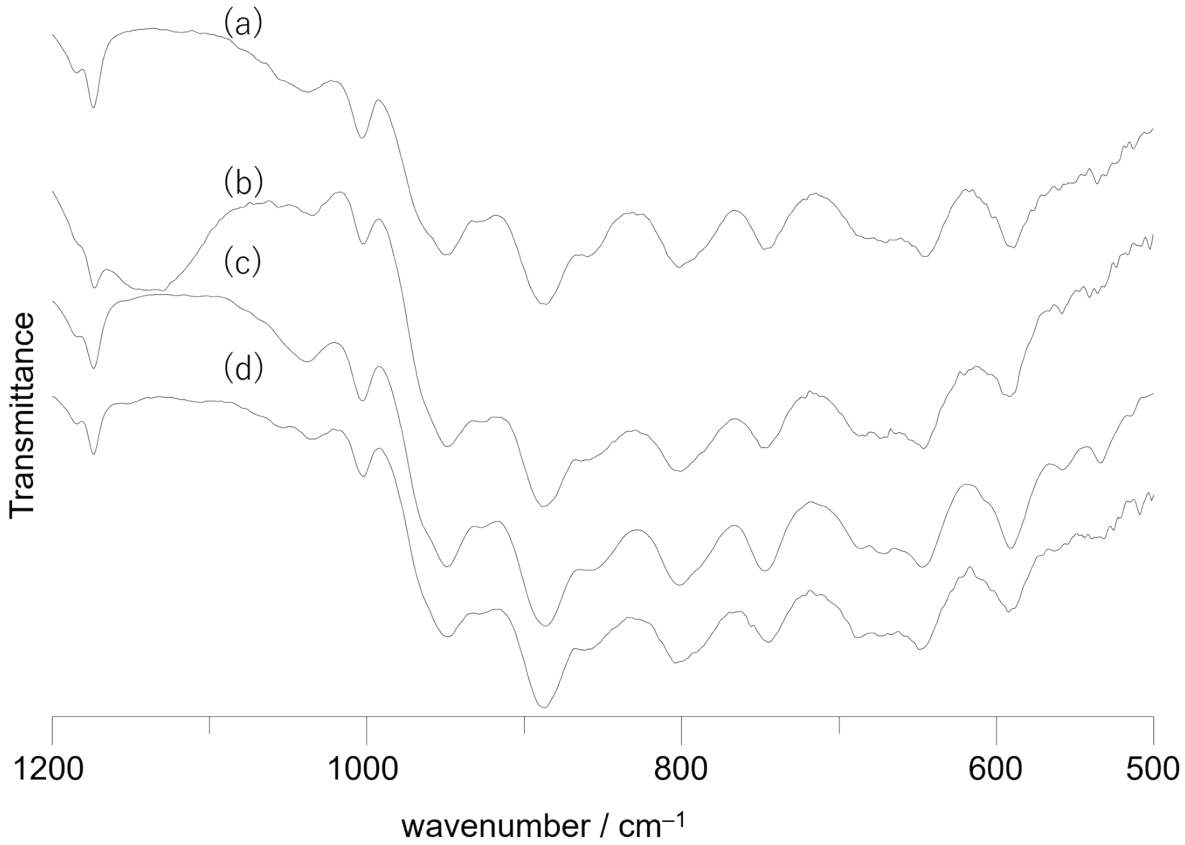

Figure S5. IR spectra of **Co13** (a) without treatment and after the treatment with (b) 10000 equiv. of dehydrated methanol, (c) 5000 equiv. of water and (d) 10000 equiv. of *tert*-butanol. with KBr method.

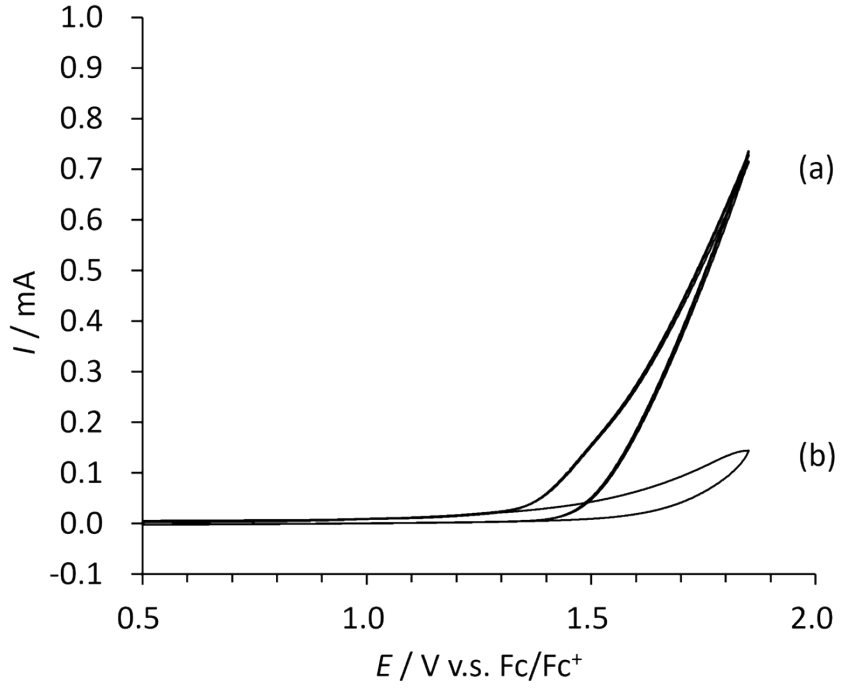

Figure S6. Cyclic voltammogram of (a) $Co(NO_3)_2$ and (b) $\{Et_4N\}_4[V_4O_{12}]$ in the presence of 39000 equiv. and 18000 equiv. of methanol, respectively.

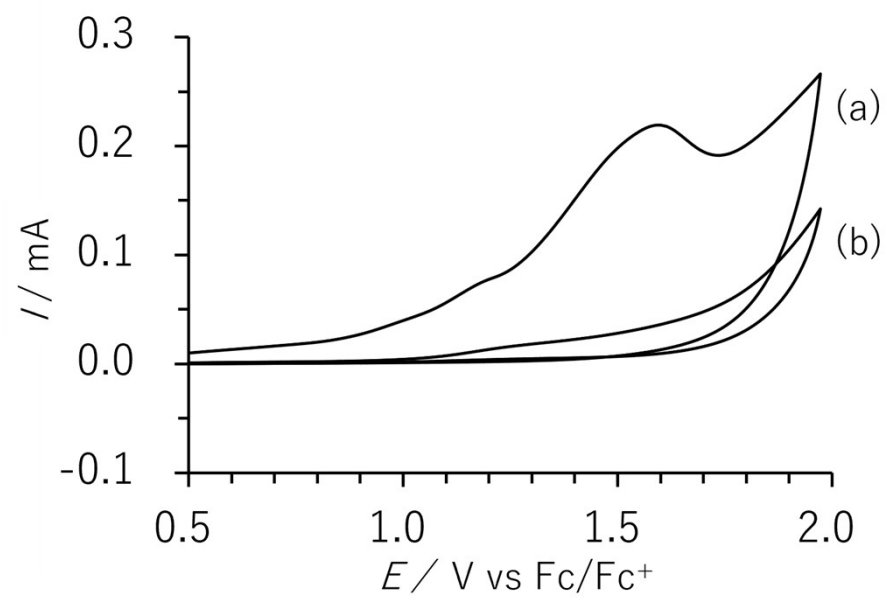

Figure S7. (a) First and (b) second scan of cyclic voltammogram of **Co13** in the presence of 3000 equiv. of methanol.

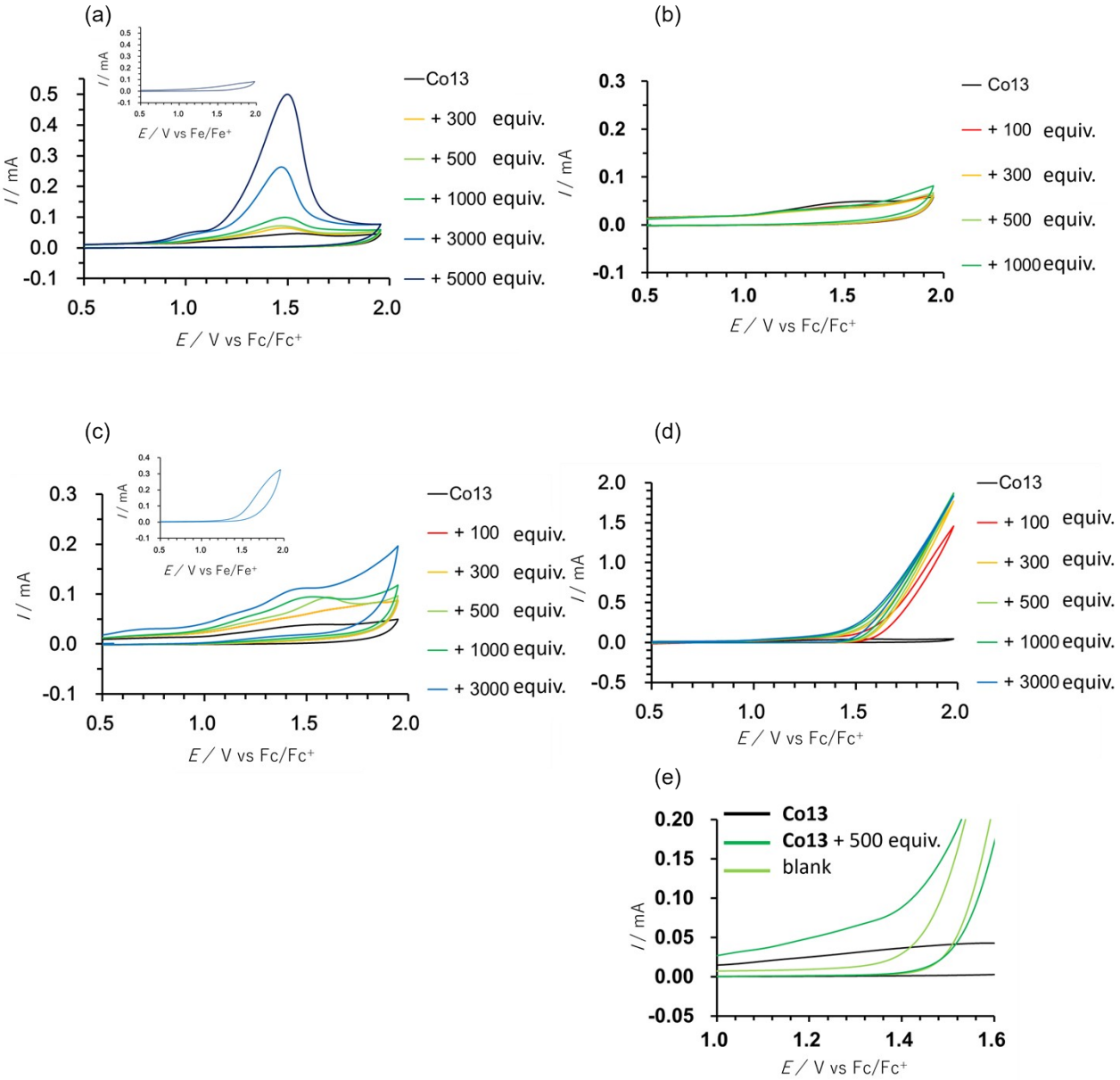

Figure S8. First cycle of cyclic voltammograms of **Co13** in the presence of (a) water, (b) tert-butanol, (c) 2-butanol and (d) benzyl alcohol The insertion represents voltammograms in the presence of additives without **Co13**. (e) The expansion of the voltammogram of **Co13** without alcohol, **Co13** with 500 equiv. of alcohol and without **Co13** in the presence of the same amount of alcohol as that with **Co13** (blank).

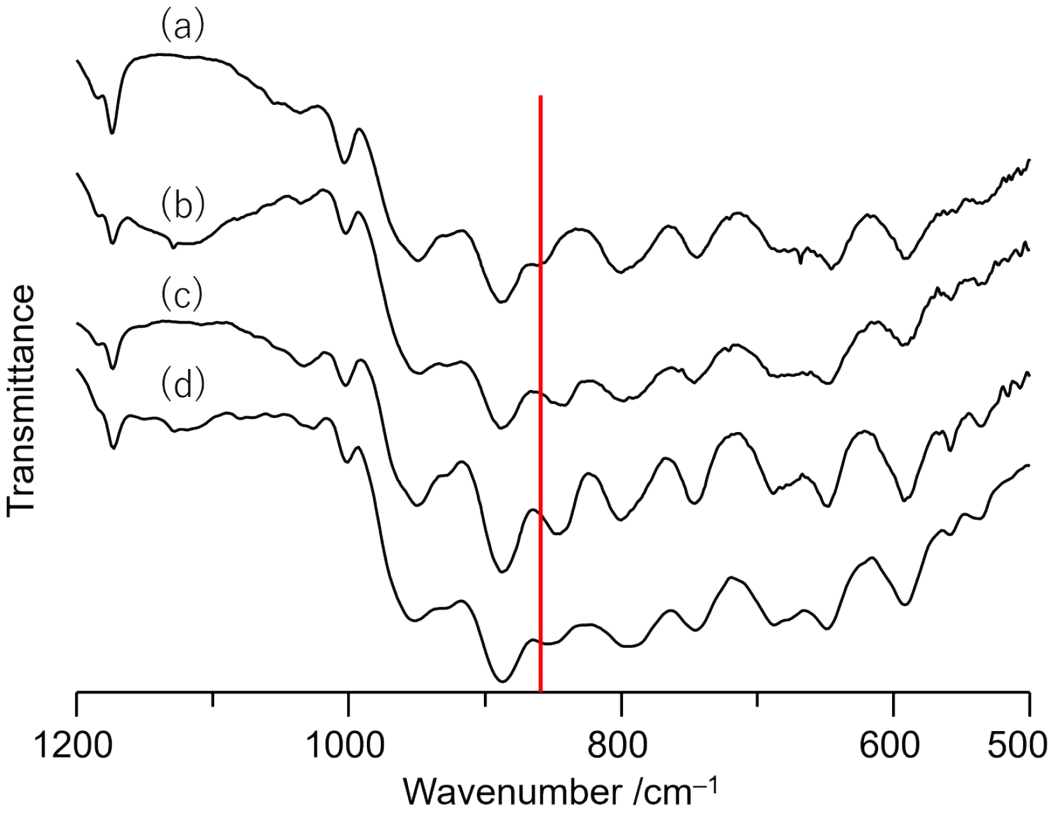

Figure S9. IR spectra of **Co13** (a) before and after the treatment with 10000 equiv. of (b) dehydrated 1-butanol, (c) dehydrated 2-butanol and (d) distilled benzyl alcohol with KBr method. The red line represents peak position at 860 cm^{-1}.

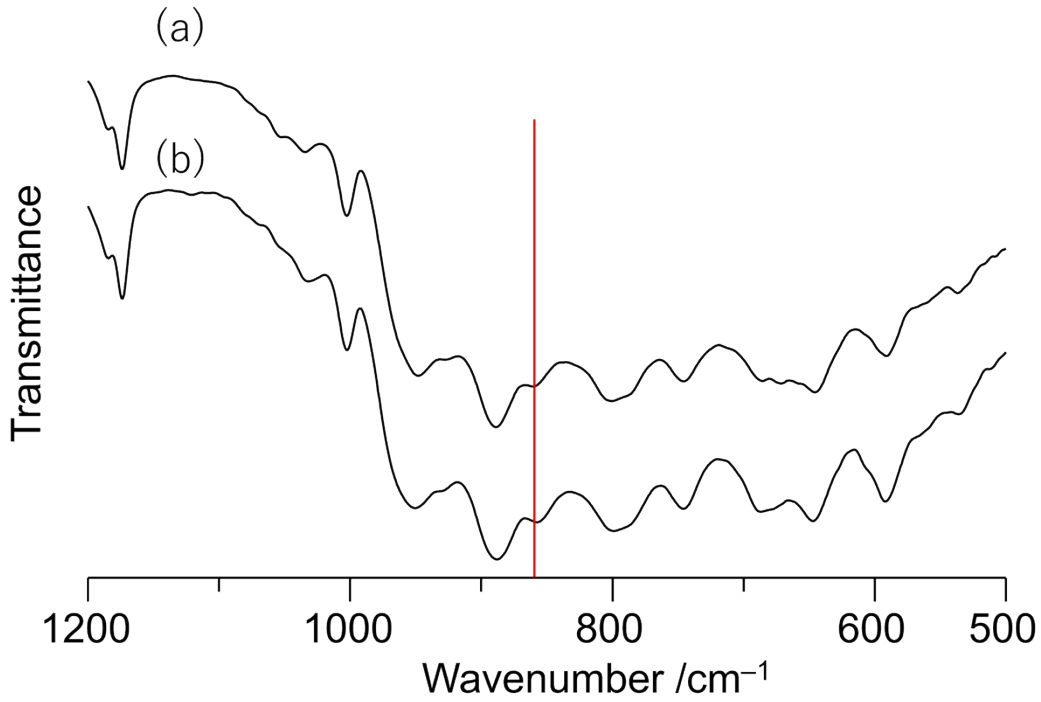

Figure S10. IR spectra of **Co13** (a) before and (b) after the treatment with 500 equiv. of TBHP with KBr method. Peak at 860 cm^{-1} was slightly shifted after the treatment. The red line represents peak position at 860 cm^{-1}.

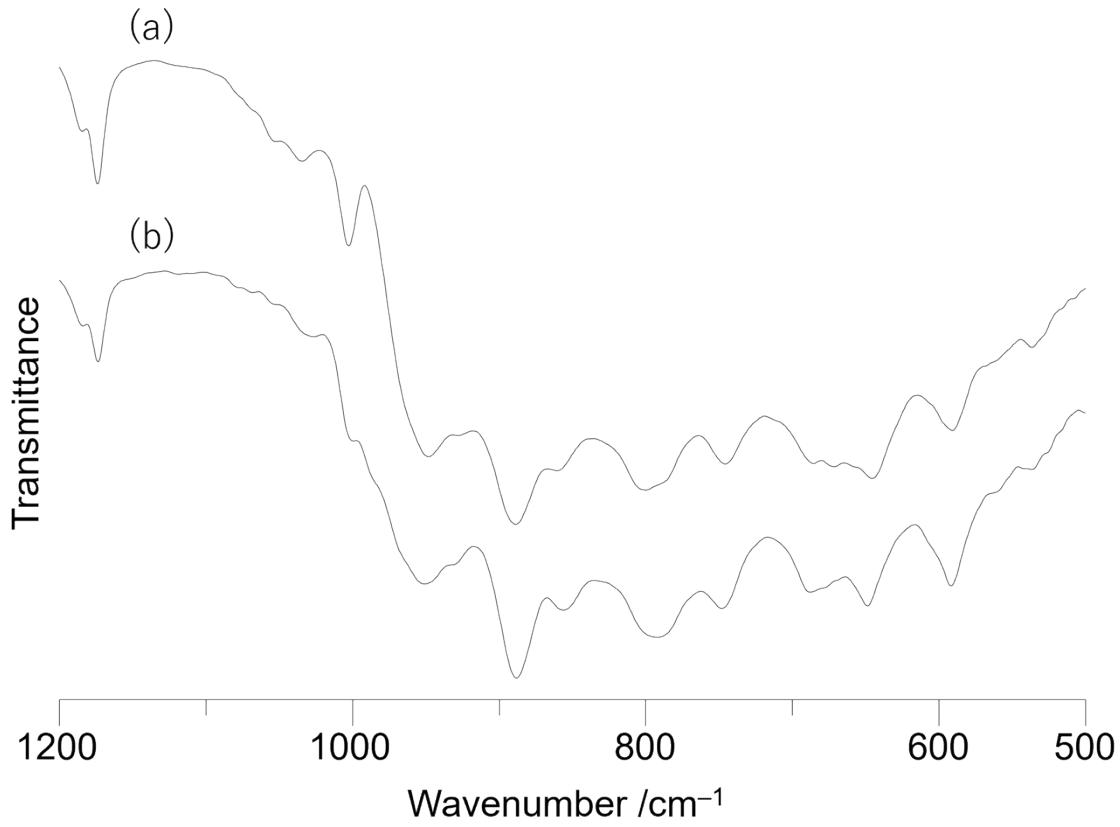

Figure S11. IR spectra of **Co13** (a) before and (b) after the oxidation of diphenyl methanol.

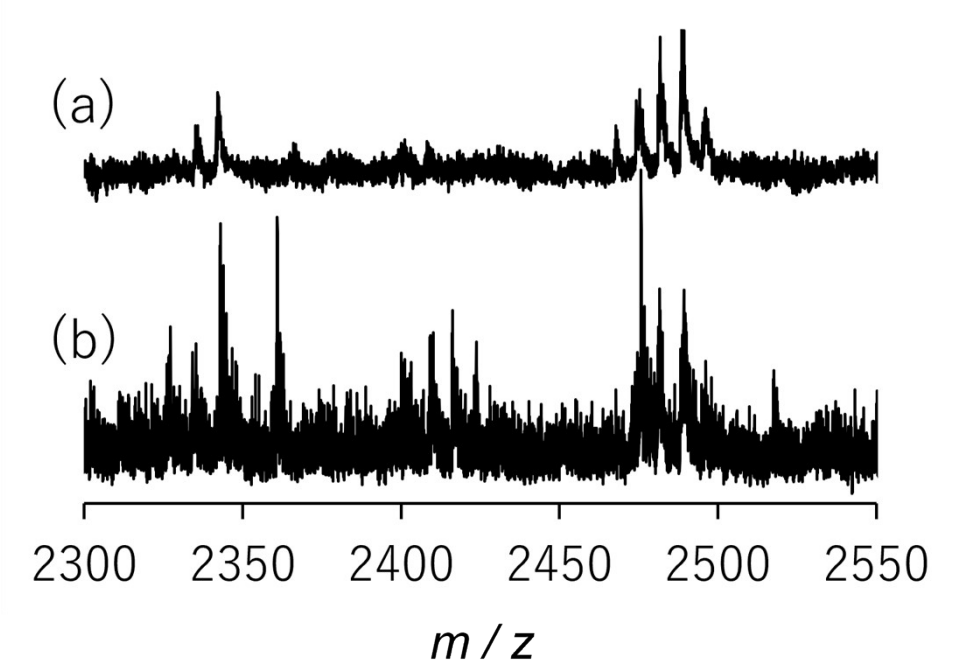

Figure S12. Electrospray ionization mass spectra of (a) **Co13** and (b) retrieved catalyst collected after the oxidation of diphenyl methanol. Spectra was measured in acetonitrile. Peak sets at 2342, 2362, 2404, 2418, 2425, 2475, 2482, 2489, and 2496 were assignable to $\{(Et_4N)(HEt_3N)_{11}[Co_{13}(OH)_6(OMe)_6V_{24}O_{72}]\}^{2+}$, $\{(Et_4N)_4(HEt_3N)_8[Co_{13}(OH)_9(OMe)_3V_{24}O_{72}]\}^{2+}$, $\{(Et_4N)_8(HEt_3N)_4[Co_{13}(OH)_{11}(OMe)V_{24}O_{72}]\}^{2+}$, $\{(Et_4N)_8(HEt_3N)_4[Co_{13}(OH)_{10}(OMe)_2V_{24}O_{72}]\}^{2+}$, $\{(Et_4N)_8(HEt_3N)_4[Co_{13}(OH)_9(OMe)_3V_{24}O_{72}]\}^{2+}$, $\{(Et_4N)_{12}[Co_{13}(OH)_9(OMe)_3V_{24}O_{72}]\}^{2+}$, $\{(Et_4N)_{12}[Co_{13}(OH)_8(OMe)_4V_{24}O_{72}]\}^{2+}$, $\{(Et_4N)_{12}[Co_{13}(OH)_7(OMe)_5V_{24}O_{72}]\}^{2+}$, $\{(Et_4N)_{12}[Co_{13}(OH)_6(OMe)_6V_{24}O_{72}]\}^{2+}$, respectively.

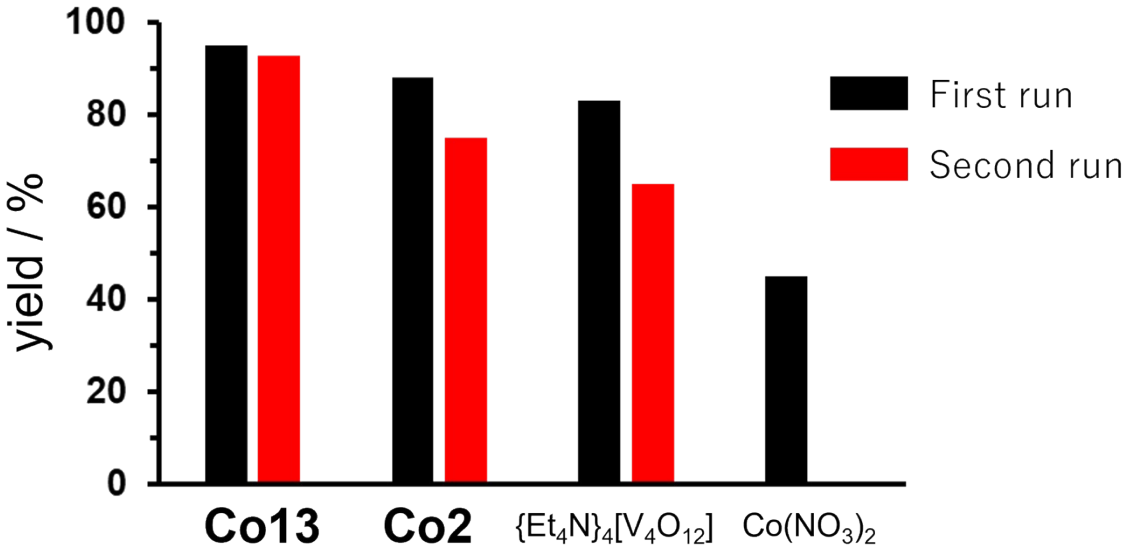

Figure S13. Reactivity of the catalysts. Back and red bars represent first and second run of the catalytic reaction.

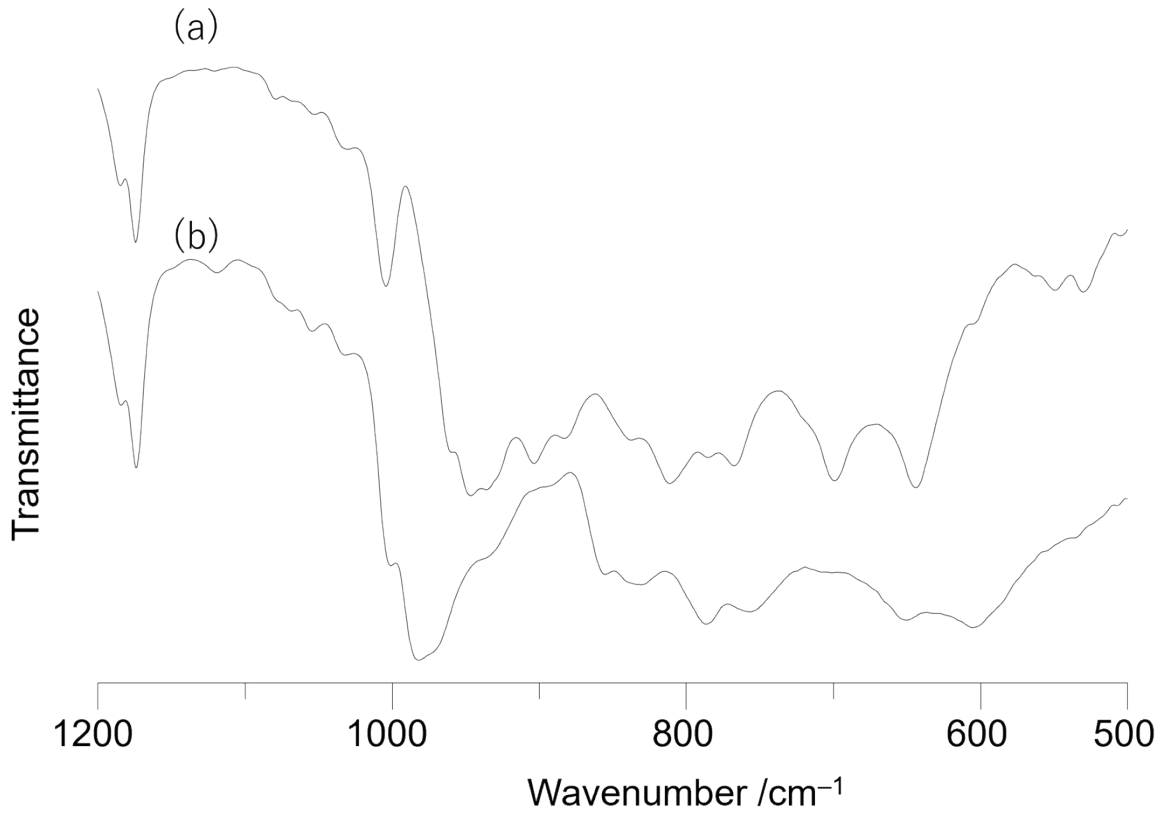

Figure S14. IR spectra of **Co** (a) before and (b) after the oxidation of diphenyl methanol.

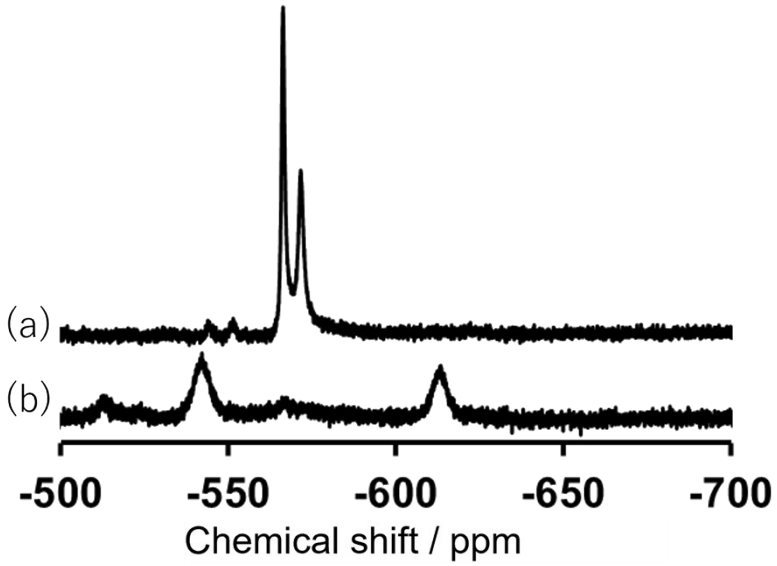

Figure S15. ^{51}V NMR spectra of $[V_4O_{12}]^{4-}$ (a) before and (b) after the oxidation of diphenyl methanol.